Imaging of Oligonucleotide-Metal Complexes by Scanning Tunneling Microscopy

Yun Kim,† Eric C. Long,‡ Jacqueline K. Barton,*,‡ and Charles M. Lieber*,†

Department of Chemistry, Harvard University, 12 Oxford Street, Cambridge, Massachusetts 02138, and Division of Chemistry and Chemical Engineering, California Institute of Technology, Pasadena, California 91125

Received August 13, 1991. In Final Form: October 2, 1991

Scanning tunneling microscopy (STM) has been used to image synthetic oligonucleotide duplexes alone or with an intercalatively bound metal complex with submolecular resolution. The sizes of 12 and 24 base pair (bp) oligonucleotides determined from STM images are in agreement with expected values, and images of isolated duplexes resolve the two nucleotide strands of these molecules. In addition, images of the 12-bp duplex in the presence of bis(9,10-phenanthrenequinone diimine)(2,2'-bipyridyl)rhodium(III) exhibit a new structural feature at 14 Å from the 12-bp duplex end. This new feature corresponds well to the metal binding sites determined from DNA cleavage and molecular modeling studies. These results indicate that STM can be used to image directly transition-metal complexes bound to DNA and thus suggest that metal complexes bound specifically to biological and other macromolecules could serve as useful labels in STM structural studies.

Introduction

Considerable effort has recently been directed toward using scanning tunneling microscopy (STM) to characterize the structures of biological macromolecules[1-22] since this technique can in principle provide atomic resolution structural data under close to physiological conditions. Reported STM investigations of nucleic acids have indeed shown great promise,[1-14] although it is apparent that this technique is not yet capable of providing reproducible and unambiguous visualization of the structures of biological macromolecules. To explore further the limits of STM as a technique for characterizing the structures of biopolymers and macromolecular assemblies, we have taken an approach that involves the study of synthetic oligonucleotide duplexes with transition-metal complexes bound by intercalation at selected positions. There are two key advantages of this approach. First, the sizes of the synthetic duplexes, which vary from 12 to 24 base pairs in this study, are well-defined and can be systematically altered. Lindsey and co-workers[8,9] have also investigated DNA fragments in their studies of sonicated calf thymus DNA, although herein we use much shorter DNA fragments (i.e., 12-24 vs 146 base pairs) that are synthesized to a specific length. Second, and perhaps of greater importance, electronically distinct metal probes can be attached to specific sites on the duplexes. Since the origin of STM contrast in images of macromolecules adsorbed on surfaces is not yet well understood, attachment of electronically distinct groups is expected to help elucidate this problem.

Experimental Methods

All of the oligonucleotides utilized in this study were synthesized on a Pharmacia Gene Assembler using β-cyanoethyl phosphoramidites and were purified by HPLC. The stock solutions of purified 12 and 24 base pair (bp) duplexes were 42 and 55 μM, respectively, and were buffered at pH 7.2 with 25 mM sodium cacodylate. The duplex-metal complex solutions contained equimolar (based on duplex) rhodium. The preparation of the rhodium metal complex used in this study has been described previously.[23-25] Aliquots of the stock solutions were diluted to between 0.1 and 1 μM prior to their deposition onto the surface substrate.

Samples were prepared for imaging by placing a 1-2 μL drop of duplex or duplex-metal solution onto a cleaved surface of highly oriented pyrolytic graphite (A. W. Moore, Union Carbide, Parma, OH). The solution was allowed to stand on the surface for ca. 10 min, after which time the remaining aqueous solution was removed. The surface was then immediately covered with oil to prevent dehydration of the duplexes as described elsewhere.[6] Solutions that were allowed to dry on the graphite yielded irreproducible results.

† Harvard University.
‡ California Institute of Technology.

(1) Travaglini, G.; Rohrer, H.; Amrein, M.; Gross, H. *Surf. Sci.* **1987**, *181*, 380.
(2) Lindsay, S. M.; Barris, B. *J. Vac. Sci. Technol. A* **1988**, *6*, 544.
(3) Beebe, T. P.; Wilson, T. E.; Ogletree, D. F.; Katz, J. E.; Balhorn, R.; Salmeron, M. B.; Siekhaus, W. J. *Science* **1989**, *243*, 370.
(4) Amrein, M.; Durr, R.; Stasiak, A.; Gross, H.; Travaglini, G. *Science* **1989**, *243*, 1708.
(5) Lee, G.; Arscott, P. G.; Bloomfield, V. A.; Evans, D. F. *Science* **1989**, *244*, 475.
(6) Arscott, P. G.; Lee, G.; Bloomfield, V. A.; Evans, D. F. *Nature* **1989**, *339*, 484.
(7) Arscott, P. G.; Bloomfield, V. A. *Ultramicroscopy* **1990**, *33*, 127.
(8) Lindsay, S. M.; Thundat, T.; Nagahara, L.; Knipping, U.; Rill, R. L. *Science* **1989**, *244*, 1063.
(9) Lindsay, S. M.; Nagahara, L. A.; Thundat, T.; Knipping, U.; Rill, R. L.; Drake, B.; Prater, C. B.; Weisenhorn, A. L.; Gould, S. A. C.; Hansma, P. K. *J. Biomol. Struct. Dyn.* **1989**, *7*, 279.
(10) Nagahara, L. A.; Thundat, T.; Oden, P. I.; Lindsay, S. M. *Ultramicroscopy* **1990**, *33*, 107.
(11) Cricenti, A.; Selci, S.; Felici, A. C.; Generosi, R.; Gori, E.; Djaczenko, E.; Chiarotti, G. *Science* **1989**, *245*, 1226.
(12) Dunlop, D. D.; Bustamante, C. *Nature* **1989**, *342*, 204.
(13) Keller, D.; Bustamante, C.; Keller, R. W. *Proc. Natl. Acad. Sci. U.S.A.* **1989**, *86*, 5356.
(14) Driscoll, R. J.; Youngquist, M. G.; Baldeschwieler, J. D. *Nature* **1990**, *346*, 294.
(15) Baro, A. M.; Miranda, R.; Alaman, J.; Garcia, N.; Binnig, G.; Rohrer, H.; Gerber, Ch.; Carrascosa, J. L. *Nature* **1987**, *315*, 253.
(16) Stemmer, A.; Reichelt, R.; Engel, A.; Rosenbusch, J. P.; Ringger, M.; Hidber, H. R.; Guntherodt, H.-J. *Surf. Sci.* **1987**, *181*, 394.
(17) Zasadzinski, J. A. N.; Schneir, J.; Gurley, J.; Elings, V.; Hansma, P. K. *Science* **1988**, *239*, 1013.
(18) Fisher, K. A.; Yanagimoto, K. C.; Whitfield, S. L.; Thomson, R. E.; Gustafsson, M. G. L.; Clarke, J. *Ultramicroscopy* **1990**, *33*, 117.
(19) Smith, D. P. E.; Bryant, A.; Quate, C. F.; Rabe, J. P.; Gerber, Ch.; Swalen, J. D. *Proc. Natl. Acad. Sci. U.S.A.* **1987**, *84*, 969.
(20) Fuchs, H.; Schrepp, W.; Rohrer, H. *Surf. Sci.* **1987**, *181*, 391.
(21) Horber, J. K. H.; Lang, C. A.; Hansch, T. W.; Heckl, W. M.; Mohwald, H. *Chem. Phys. Lett.* **1988**, *145*, 151.
(22) Wu, X. L.; Lieber, C. M. *J. Phys. Chem.* **1988**, *92*, 5556.
(23) Pyle, A. M.; Long, E. C.; Barton, J. K. *J. Am. Chem. Soc.* **1989**, *111*, 4520.
(24) Pyle, A. M.; Morii, T.; Barton, J. K. *J. Am. Chem. Soc.* **1990**, *112*, 9432.
(25) Pyle, A. M. Ph.D. Thesis, Columbia University, 1989.

0743-7463/92/2408-0496$03.00/0

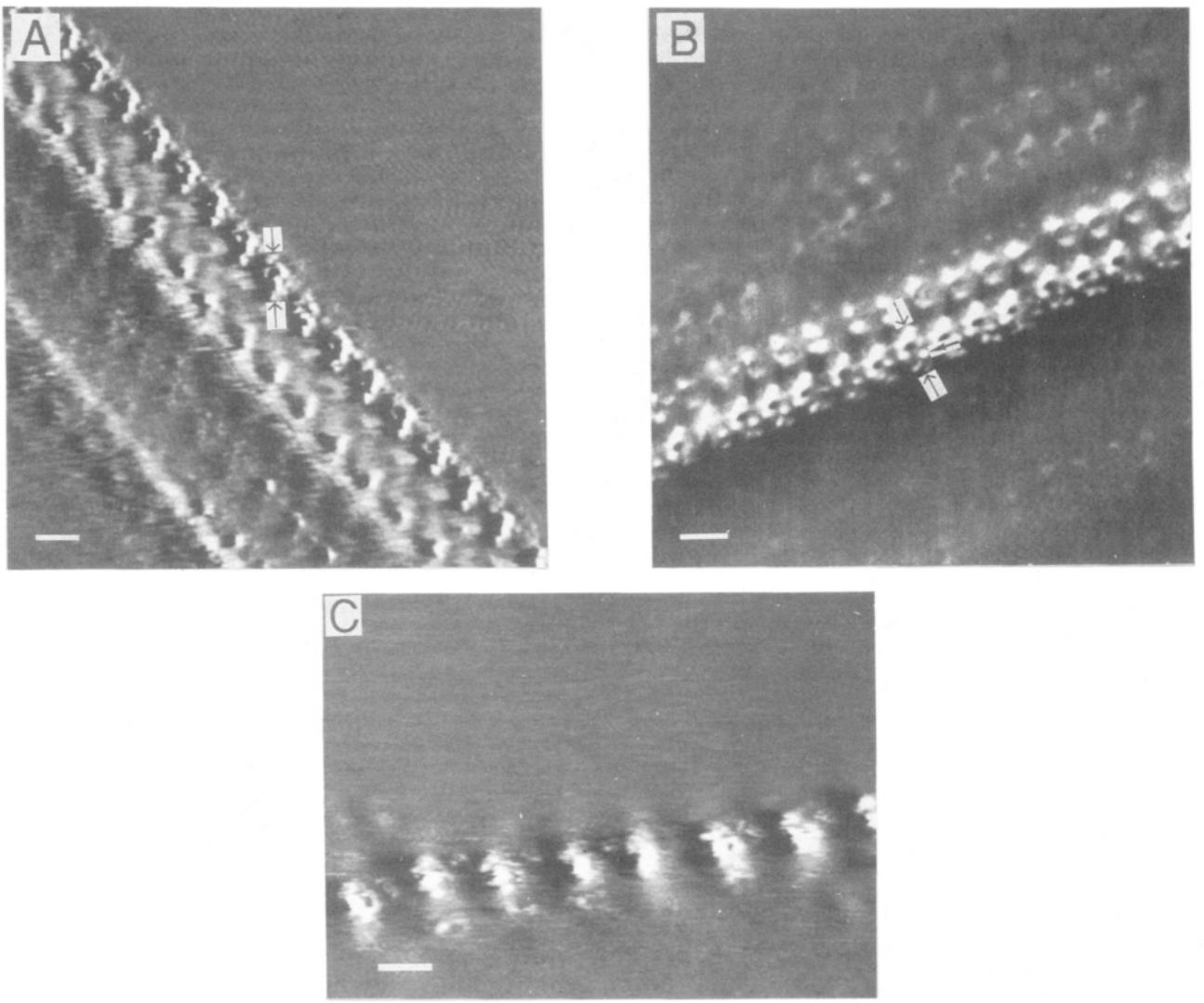

Figure 1. (A) 540 × 540 Å^2 gray-scale image of 12-bp duplexes recorded with a bias voltage of 100 mV and a tunneling current of 1.0 nA. The duplexes were adsorbed onto the graphite surface from a 0.3 μM solution. (B) 420 × 420 Å^2 image of 12-bp–Rh(phi)$_2$(bpy)$^{3+}$ complexes recorded with a bias voltage of 100 mV and a tunneling current of 1.0 nA. The duplex–rhodium complexes were deposited from a 0.3 μM solution. The light arrows in parts A and B indicate the ends of a single duplex; the heavy arrow in part B highlights the rhodium metal complex. Ghost images of the 12-bp duplexes due to multiple tunneling tips are also observed below and above the rows of duplexes in parts A and B, respectively. (C) A lower resolution image of 12-bp duplexes recorded using similar conditions as in part A; no ghost features are observed in these data. The data in parts A and B have not been filtered. The white bars in the lower left corner of parts A, B, and C correspond to 40 Å.

All of the STM images were recorded with a commercial instrument (Nanoscope, Digital Instruments, Inc., Santa Barbara, CA) operated in the constant current mode using platinum–iridium alloy (80%–20%) tips. The tips were mechanically sharpened prior to imaging. The images were acquired with bias voltages from −300 to −100 and +60 to +500 mV; over this range of bias voltages, the images were similar. Unless otherwise stated the images presented in this paper correspond to raw, unfiltered data. Additional experimental details and procedures have been described elsewhere.[26]

Photoactivated cleavage of the oligonucleotide–metal complexes was accomplished by irradiation of the solution for 4 min at 313 nm using a 1000-W Hg/Xe lamp.[27] The cleavage histograms were determined from the analysis of the cleavage pattern by 20% polyacrylamide gel electrophoresis.[23,24,27]

The molecular models of the duplex–metal complexes were constructed using Macromodel (V2.5, W. C. Still, Columbia University) by inserting an intercalation site[28] into a B-form helix and docking the rhodium complex with the metal ligand intercalatively stacked.[25]

Results and Discussion

Oligonucleotide–Metal Complexes. The self-complementary oligonucleotide used in this study, d(CGCTTATAAGCG)$_2$, and the 24 base pair (24-bp) oligonucleotide d(CATGCCAGCATGCATGCATGCATG) and its complement were chosen to promote selective binding by a metal complex at a particular base pair step within the duplex structure. The metal complex used in this study, Rh(phi)$_2$bpy^{3+} (phi, 9,10-phenanthrenequinone diimine; bpy, 2,2′-bipyridyl), binds avidly to DNA by intercalation and upon irradiation promotes efficient and selective DNA strand scission.[23,24,27]

Imaging the 12-bp Duplex. Images of the 12-bp duplex and 12-bp–metal complex recorded using various conditions are shown in Figure 1. Figures 1A,C are typical of the results obtained for concentrations of duplex less than 1 μM. In these images the duplexes appear to order along linear defects on the graphite surface (possibly step edges) with the helix axes oriented at an approximately

(26) (a) Wu, X. L.; Lieber, C. M. *Science* **1989**, *243*, 1703. (b) Wu, X. L.; Wang, Y. L.; Zhang, Z.; Lieber, C. M. *Science* **1990**, *248*, 1211.
(27) Uchida, K.; Pyle, A. M.; Morii, T.; Barton, J. K. *Nucleic Acids Res.* **1989**, *17*, 10259.
(28) Wang, A. H. J.; Nathans, J.; van der Marel, G. A.; van Boom, J. H.; Rich, A. *Nature* **1978**, *276*, 471.

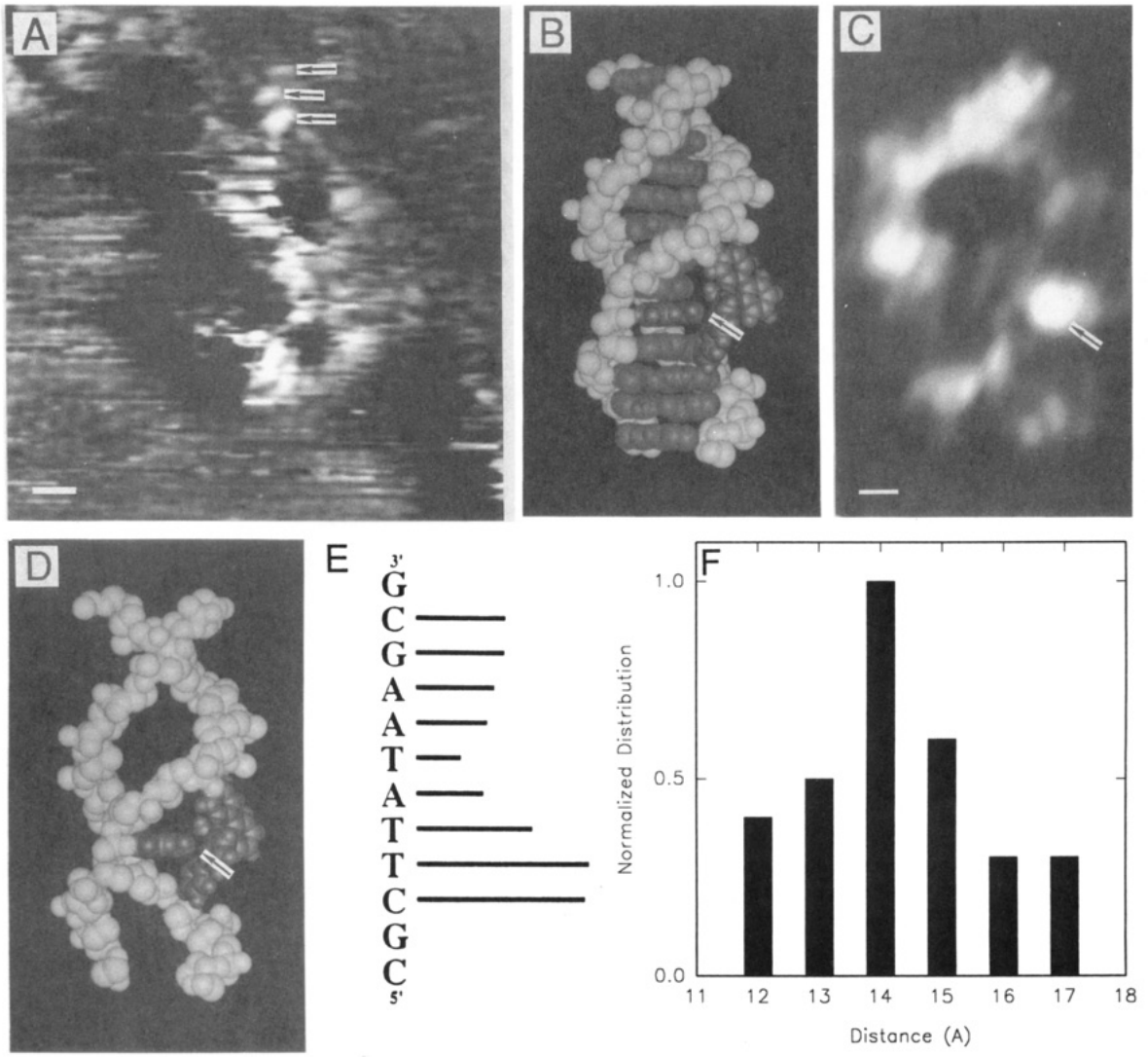

Figure 2. (A) A high-resolution image of a single 12-bp duplex recorded under conditions similar to Figure 1; the white scale bar corresponds to 5 Å. The three arrows denote atomic structure with a spacing of 3.2 Å. The shadow to the left of the duplex is due to the inability of the feedback loop to track the height change when scanning across the duplex from right to left. (B) Molecular model of the B-form 12-mer with $Rh(phi)_2bpy^{3+}$ shown intercalated at its preferred site based upon the cleavage results. The sugar–phosphate backbone is shown in white, the base pairs in dark gray, and the metal complex in light gray; the complex is indicated with an arrow. (C) An image of a single 12-bp–$Rh(phi)_2(bpy)^{3+}$ complex; the white scale bar corresponds to 4 Å. The arrow highlights the new topological feature observed only in images of duplexes that are complexed with metal; this feature is 14 Å from the end of the duplex. (D) Molecular model of the duplex with bound $Rh(phi)_2bpy^{3+}$ shown without the Watson–Crick base pairs. (E) Histogram indicating the positions of cleavage and quantifying the relative intensities at different sites based upon measurements of photoactivated cleavage by the rhodium complex. (F) Histogram of the experimentally determined metal-binding-site to duplex-end distance.

45° angle relative to the direction of the defect. Images of the 12-bp–metal complex (e.g., Figure 1B) also show that the duplex–metal system orders along graphite defects with the helix axis at an angle to the defect direction. The average lengths/widths of the 12-bp duplexes and 12-bp–metal complexes determined from our images are 38 ± 2/22 ± 1 and 39 ± 2/23 ± 2 Å, respectively (Table I). The vertical corrugation of the duplexes in these images ranged from 10 to 15 Å. This corrugation is smaller than predicted based on an ideal DNA helix diameter (i.e., 23 Å). This corrugation is not, however, inconsistent with a surface-adsorbed duplex since surface adsorption and partial dehydration are expected to flatten the duplex and thus reduce its observed corrugation. In addition, since DNA is not "metallic", it is expected that the z response (i.e., the corrugation) of the STM will be reduced when scanning over this macromolecule. The orientation of the 12-bp duplexes contrasts previous studies of large DNA fragments[5,6,13] in which the DNA was proposed to order with the helix axis parallel to linear defects. We believe that the nonparallel orientation, feasible with small oligonucleotides, is advantageous since it is possible that linear defects enforce a rigid conformation on the parallel-oriented DNA.

We have also carried out extensive blank experiments to rule out the possibility that the features observed in our images are due to surface defects and not the oligonucleotides. Recent reports[29] have shown that a variety of defects can be observed on the surface of graphite; however, these features are generally larger in size than the specific 12- and 24-bp oligonucleotides we have studied. We thus believe that it is unlikely that such defects could explain our observed results,[29c] especially since the feature size we observe changes reproducibly with the duplex size (see below). Images of blank solutions containing the cacodylate buffer or the buffer and metal complex deposited on graphite surfaces also did not show the features assigned

(29) (a) Clemmer, C. R.; Beebe, T. P. *Science* **1991**, *251*, 640. (b) Chang, H.; Bard, A. J. *Langmuir* **1991**, *7*, 1143. (c) Images recorded on graphite in our laboratory since 1987 have not exhibited features like those observed when the 12- and 24-bp duplexes are adsorbed on the graphite surface: Kim, Y.; Wu, X. L.; Kelty, S. P.; Lieber, C. M. Unpublished results.

to the 12-bp duplex when studied for a comparable length of time at graphite linear defects. In addition, extensive imaging studies of calf thymus DNA carried out over an 8-month period using conditions similar to those employed for these duplex studies *did not* show the features that we attribute to the duplexes (Figures 1–3). Hence, we strongly believe that these features represent images of the duplexes and are not due to artifacts of the graphite surface.[29]

Isolated duplexes, which are observed when depositing the DNA from dilute solutions, also can be reproducibly imaged with high resolution. A close-up image of one 12-bp duplex clearly shows the two nucleotide strands and the atomic structure of the graphite substrate (Figure 2A). This image corresponds to raw data and has not been filtered. The length and width of this duplex, 37 and 22 Å, respectively, are in good agreement with the dimensions expected for a B-conformation 12-bp oligonucleotide fragment (Table I). We also find structure with a spacing of 3.2 Å that may correspond to the base pairs (3.4 Å separation) or the phosphate backbone. This near atomic resolution structure is not always observed, however, and thus we cannot definitively assign it at the present time.

The Metal Binding Site. We believe that another significant aspect of this work lies in our studies of the oligonucleotides with bound metal complexes. Notably, images of isolated 12-bp duplexes complexed with Rh(phi)$_2$(bpy)$^{3+}$ show a new topographical feature centered 14 ± 2 Å from the end of the duplex (Figures 1B and 2C). The uncertainty in this value may reflect variations in oligonucleotide length due to variable hydration[2,3,5–9] or metal binding to a distribution of base pair sites. We only observe this new feature in images of the duplex–metal complex and have not observed reproducibly similar features in images of the duplex without the bound metal. The average position of this raised feature does agree well with the favored metal binding site determined through photoactivated cleavage of the oligonucleotide, as indicated in the histogram (Figure 2E). The photocleavage histogram exhibits a significantly wider distribution of cleavage sites than observed in our quantitative analysis of the binding site distribution shown in Figure 2F. There are several possible explanations for these differences. For example, cleavage of DNA does not necessarily occur at the specific site of intercalation and thus the photoactivated cleavage assay should yield a distribution that is broader than the actual binding site distribution.[23–25,27] It is also likely that the metal binding constants differ in solution versus on a surface. While additional studies will be needed to resolve better these differences, it is nevertheless evident that the cleavage and STM determined binding site distributions are similar.

Hence, we propose that the new features observed in our images correspond to a direct visualization of the bound metal complex. Indeed, a computer-generated model of the duplex–Rh(phi)$_2$(bpy)$^{3+}$ complex (Figure 2B) is similar to the STM image of this system. Perhaps even more remarkable is the similarity of the image to a model showing only the metal complex and sugar–phosphate backbone (Figure 2D). Comparisons of the STM images to the van der Waals surface of the molecular model should be made with caution since the mechanism of imaging is not yet understood. The enhanced image contrast for the phosphate backbone relative to the base pairs is consistent, however, with a larger relative reduction in the graphite surface potential by the charged phosphate backbone compared to the neutral base pairs.[14,30] The fact that the phosphate backbone and charged (3+) metal complex exhibit similar contrast in images recorded with negative (−100 to −300 mV) and positive (60 to 500 mV) bias voltages is also consistent with this explanation,[30] although additional studies will be needed to understand fully the mechanism of imaging in these systems.

Table I. Summary and Comparison of the Duplex and Duplex–Rhodium Complex Dimensions Determined from Analysis of STM Images,[a] Molecular Modeling,[b] or Idealized B-Form DNA[c]

oligonucleotide	length, Å	width, Å	metal to duplex end
	5′-dCGCTTATAAGCG Alone		
STM	38 ± 2	22 ± 1	
MM	40 (37)	20.4 (17.4)	
B	40.6	23	
	5′-dCGCTTATAAGCG + Rh(phi)$_2$bpy^{3+}		
STM	39 ± 2	23 ± 2	14 ± 2
MM	42.8 (39.8)	20 (17)	15.1 (13.6)
B	44.2	23	

[a] The values represent averages (mean ± standard deviation) of measurements made on at least five independent images per duplex or duplex–rhodium complex. [b] Measurements were derived from models oriented as observed in the STM images including van der Waals radii of 1.5 Å using Macromodel V2.5 (W. C. Still, Columbia University); values in parentheses indicate measured internuclear distances. The site of intercalation utilized for modeling[28] was incorporated into a B-form duplex DNA of proper nucleotide length. [c] Using a base pair repeat of 3.4 Å.

A summary of the data obtained from a number of independent images recorded for the 12-bp duplex system is given in Table I. The distances taken from the high resolution STM images and those based upon B-DNA model structures oriented comparably to the STM images are generally similar. Comparison of the overall lengths of both the metal-free and metal-bound duplexes with models shows, however, differences. The STM images yield shorter overall lengths than would be expected based upon modeling. Variations in the DNA helix repeat length, especially smaller repeat distances, have been observed in previous STM studies and have been attributed to reduced hydration of the DNA.[2,3,5–9]

Comparisons of metal-bound and metal-free duplex lengths also indicate that the duplexes and duplex–metal complexes have the same lengths within experimental error. An increase of 3.4 Å along the helix axis is expected upon intercalation, owing to the unwinding of the helix to accommodate the intercalator.[25] The observed results may reflect (i) variations in the duplex length due to hydration, (ii) a smaller than expected expansion of the oligonucleotide on intercalation, and/or (iii) an uncertainty in measurement as a result of the fraying open of the termini of these short oligonucleotides (Figure 2C). Additional studies will be needed to address these interesting points. Irrespective of these differences from ideal DNA models, our results for the 12-bp oligonucleotides containing bound rhodium complexes suggest that it is possible to image transition-metal complexes bound to DNA.

Imaging 24-bp Oligonucleotides. In addition, we have explored the generality of these results by imaging 24-bp oligonucleotides on graphite using STM. An image of 24-bp duplexes deposited onto graphite from a 0.4 μM solution is shown in Figure 3. To date, the resolution observed in images of the 24-bp oligonucleotides has been somewhat lower than that observed for the isolated 12-bp duplexes (Figure 2). A right-handed helical structure can be visualized, however, in the images of these 24-bp oligonucleotides. We believe that the lower resolution may be due to greater dehydration of these duplexes in comparison

(30) Spong, J. K.; Mizes, H. A.; LaComb, L. J.; Dovek, M. M.; Frommer, J.; Foster, J. S. *Nature* **1989**, *338*, 137.

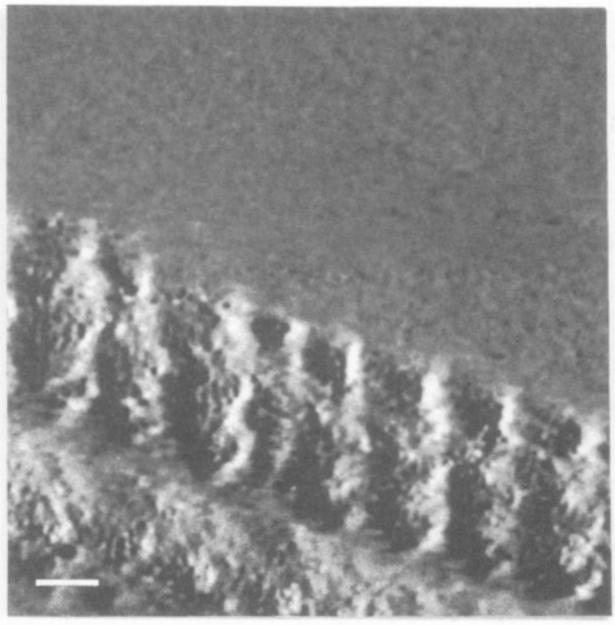

Figure 3. A 210 × 210 Å^2 image of 24-bp duplexes recorded with a bias voltage of 100 mV and a tunneling current of 1 nA. The eight duplexes in this image are oriented nearly vertical with respect to the page. The vertical corrugation of these duplexes ranges from 10 to 12 Å. The image was filtered to remove high frequency noise. The white scale bar in the lower left corner corresponds to 20 Å.

to the 12-bp system. Consistent with this proposed dehydration we find that the oligonucleotide lengths determined for the 24-bp system, ≈70 Å, are shorter than predicted for B-form DNA (80 Å). Nevertheless, it is clear from these studies of the 24-bp duplexes that the lengths of the 24- and 12-bp oligonucleotides do vary systematically in our experimental images and thus cannot be readily explained as surface defects. Hence, we conclude that the features in our images correspond to DNA.

Conclusions

In summary, STM has been used to study systematically 12- and 24-bp oligonucleotide duplexes alone or with an intercalatively bound rhodium complex. The sizes of the duplexes determined from STM images are consistent with expected values, and furthermore images of isolated 12-bp duplexes resolve the nucleotide strands of these macromolecules. In addition, images of the 12-bp duplex in the presence of $Rh(phi)_2bpy^{3+}$ exhibit a new feature that corresponds well to the metal binding site determined from DNA cleavage and molecular modeling studies.

Our work shows that it is possible using STM to probe directly transition-metal complexes bound to DNA. Transition-metal complexes bound specifically to biological molecules might therefore serve as useful labels or markers in STM structural studies. Perhaps of greater importance in the short term is that the metal complexes bound to duplexes or other macromolecules provide an ideal opportunity to probe the fundamental factors that affect electron tunneling (and hence image contrast) in these systems since the charge and electronic states of the metal complexes can be varied.[31] Such studies are critical at this time to assess whether STM can be developed into a useful technique for characterizing the structures of macromolecules.

Acknowledgment. We are grateful for the financial support of the David and Lucile Packard, A. P. Sloan, and Camille and Henry Dreyfus Foundations (C.M.L.) and the NIH (E.C.L. and J.K.B.). E.C.L. is a Fellow of the Jane Coffin Childs Memorial Fund for Medical Research.

(31) Pyle, A. M.; Rehmann, J. P.; Meshoyrer, R.; Kumar, C. V.; Turro, N. J.; Barton, J. K. *J. Am. Chem. Soc.* **1989**, *111*, 3051.